https://doi.org/10.48047/AFJBS.6.5.2024.7920-7946

AfricanJournalofBiological Sciences

Synthesis, Analysis and Biological assessment of a Novel Coumarin Azo-Dye Ligand and Its 3d Metal Complexes for Photocatalytic investigationof MB dye

H.A. Anilkumara[1], G. Krishnamurthy[*1], Malathesh Pari[1], T. Manjuraj[2], N.K. Vasantakumarnaik[1], G.Y. Akarsh[1], G. Vishnu[3]

[1]Department of P.G. Studies and Research in Industrial Chemistry, Sahyadri Science College, Kuvempu University, Shivamogga-577 203, Karnataka, India.Email: gkmnaiksahyadri@gmail.com, anilkumarhoney07@gmail.com, malathshpari@gmail.com, vasanthnaiknk77@gmail.com, akarshgy@gmail.com

[2]Department of Chemistry, Bapuji Educational Association DRM Science College, Davanagere University, Davanagere, Karnataka, India. manjuraj877@gmail.com

[3]Department of P.G. Studies and Research in Industrial Chemistry, School of Chemical Sciences, Kuvempu University, Shankaraghatta, 577 451, Karnataka, India.g.vishnu.g22@gmail.com

*Correspondence Email: gkmnaiksahyadri@gmail.com

Article History
Volume 6, Issue 5, 2024
Received: 22 May 2024
Accepted: 29 May 2024
doi:*10.48047/AFJBS.6.5.2024.7920-7946*

Abstract

A novel azo dye ligand, 7-hydroxy-4-methyl-8-[(*E*)-(6-nitro-1,3-benzothiazol-2-yl)diazenyl]-2*H*-chromen-2-one ligand (MNB)was synthesized, and has been used to synthesise Co(II), Ni(II), Cu(II) complexes. The synthesized compounds were characterized using various physicochemical and spectroscopic techniques.The biological investigation of the synthesized Schiff base ligand and its metal complexes have been determined against the bacteria (Staphylococcus aureus and Escherichia coli), fungal (A. flavous and P. anomala) and antioxidant activity using Iron chelating assay by using standard assay method.Analysis of the absorbance data revealed degradation percentages of 83%, 64% and 61% for Co(II), Ni(II) and Cu(II) complexes, respectively. These results indicate that Co(II) complex exhibit superior photodegradation efficiency compared to the Ni(II) and Cu(II) complexes for methylene blue dye.

Keywords: Azo-dye, Metal complexes, Photocatalytic activity, Antimicrobial, Molecular docking.

1. Introduction

Azo-dye molecules having (-N=N-) group that can serve as ligand in coordination chemistry and their metal complexes have gained significant attention in coordination chemistry [1-4]. The study of coordination chemistry of azo dye metal complexes involves interesting bonding interactions, spectroscopic properties and their reactivity which contributes for the development of new materials and technologies [3-4] The presence of hetero atom moieties in azo dyes has led to the discovery of numerous azo compounds and their metal complexes with remarkable medicinal properties. These compounds have found applications in various industries, including textiles, toys, leather, plastics and cosmetics [5-8]. Their low toxicity and lack of adverse effects on hyperactivity or allergic reactions make them suitable for use in paints, polymers, food, pharmaceuticals and other everyday items. Furthermore, 4-hydroxycoumarine compounds exhibit a wide range of therapeutic properties including anticoagulant [9], antibacterial [10], antifungal [11], antiviral [12], anticancer and anti-inflammatory activities [13-14]. Recent advancements have also seen the development of azo dye derivatives as HIV protease inhibitors and tyrosine kinase inhibitors. Furthermore, metal complexes of azo dyes play a significant role in the medical field as pharmaceuticals due to their potential applications in imaging, drug delivery and diagnostics. These complexes exhibit unique characteristics that make them suitable for various biomedical purposes. Consequently, the development of novel synthetic compounds with biological potency has become imperative in the global medical arena [15-16].

In the past few years, our laboratory has made significant progress in the synthesis of azo dye derivatives, their metal complexes, the electrochemical, photocatalytic detection of bio-vital molecules and the biological investigation of synthesized molecules. In highlight of these works, we are pleased to report the synthesis of a novel azo dye ligand, 7-hydroxy-4-methyl-8-[(*E*)-(6-nitro-1,3-benzothiazol-2-yl)diazenyl]-2*H*-chromen-2-one ligand (MNB) and its 3d metal complexes. Furthermore, we have successfully demonstrated the photocatalytic degradation of MB dyes using the synthesized metal complexes. Recent studies have described the synthesis and biological investigations of novel metal complexes derived from coumarin derivatives. Transition metals such as Co, Cu and Ni found in biological system.

2. Experimental Section

2.1 Materials and methods

In this synthesis, all chemicals and solvents used were of analytical grade and obtained from Sigma Aldrich and Hi-Media. The melting points of the ligand and its metal complexes were determined using DTC-967 digital melting point analyser. The carbon, hydrogen and nitrogen elemental analysis were found by using Perkin-Elmer 2400 series II CNS analyser. IR spectra were determined by FTIR spectroscopy, IR Spirit Shimadzu serial no; A224159 (Made in Japan) at Sahyadri Science College, Shivamogga, Karnataka, India. KBr pellets made by using hydrolic press and spectra were recorded in the range 350-4500 cm^{-1}. Electronic spectra were recorded in DMSO solvent using a systronics UV-Vis spectrometer 119 at Sahyadri Science College, Shivamogga. Using TMS as the internal standard, the 1H NMR spectrum was measured using Jeolanalyzer operating at 400 MHz in DMSO-d6 at Mangalore University, Mangalore. The XRD composition were analysed by using Brucker D8 advance and SEM was measured using Carl Zeiss model-EVO LS 15. The synthesized compounds LC-MS composition were identified MS model Acquity UPLC made in USA at Mysuru.

2.2 Synthesis of azo dye ligand (MNB)

A two-step synthesis was employed to produce an azo dye ligand, commencing with the synthesis of 7-hydroxy-4-methyl coumarin. This was through the addition of equimolar amounts of resorcinol (5g) and ethylacetoacetate (5 mL) in the presence of concentrated sulfuric acid (50 mL). The reaction mixture was cooled to 0-5 ℃ using an ice salt bath and allowed to undergo reaction for 10 hrs at room temperature. Subsequently, the reaction mixture was carefully poured into ice-cold water. After the resulting solution was basified with sodium hydroxide, The progress of the reaction was monitored by TLC (Ethyl acetate: Petroleum ether, 1:3).This precipitate was then collected through filtration and washed with distilled water. Confirmation of the obtained compound was determined through melting point, which was found to be 188℃. The synthesis of 7-hydroxy-4-methyl coumarin was effectively carried out.

In the second step, a mixture was prepared by combining 20 mL of distilled water, 4 mL of concentrated hydrochloric acid, and 2 mmol of 2-amino-6-nitrobenzothiazole to form a diazonium solution. Subsequently, a cold aqueous solution of sodium nitrite (2 Mmol) dissolved in 3 mL of concentrated sulfuric acid was added dropwise with stirring to the previously mentioned solution, which had been cooled to a temperature range 0-5℃ using an ice bath, following this addition, a cold solution of 7-hydroxy-4-methyl coumarin (2 Mmol) in alkaline media was added, the resulting mixture was stirred approximately two hours at the same

temperature, keeping the pH in the range of 7-8. The progress of the reaction was monitored by TLC (Ethyl acetate : Petroleum ether, 1:3). Then poured into ice cold water, the precipitate was filtered and washed with distilled water and recrystallised with ethanol. Yield 69 %, to get 7-hydroxy-4-methyl-8-[(*E*)-(6-nitro-1,3-benzothiazol-2-yl)diazenyl]-2*H*-chromen-2-one.The reaction pathway of the above procedure is represented in Scheme 1.

Step 1:

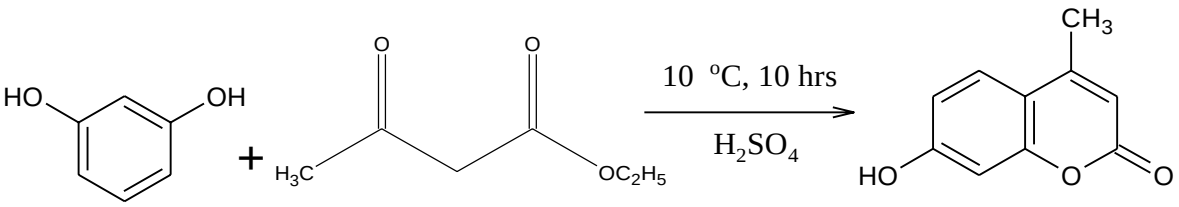

Step 2:

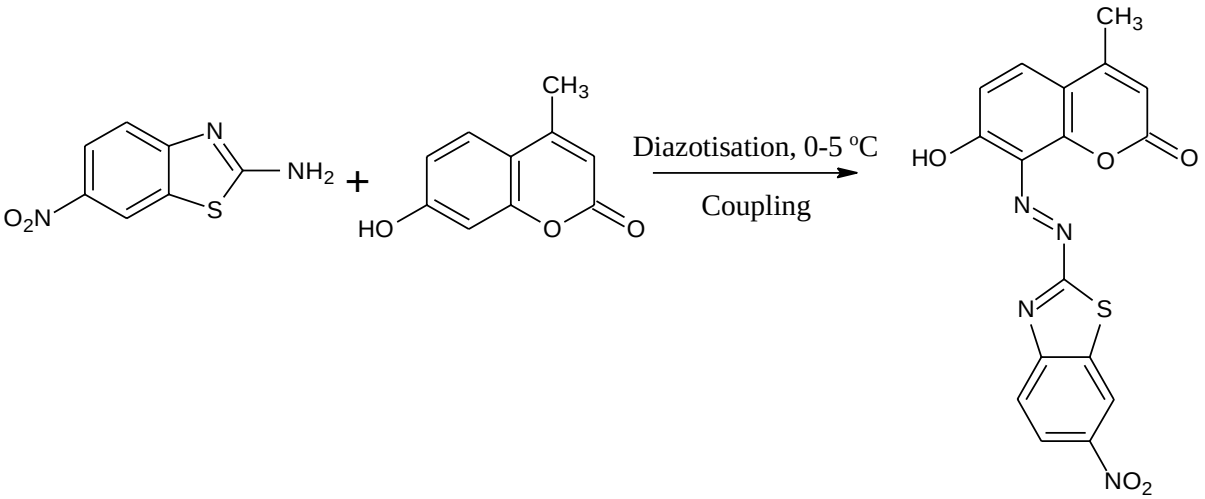

Scheme 1. Synthesis of azo dye 7-hydroxy-4-methyl-8-[(*E*)-(6-nitro-1,3-benzothiazol-2-yl)diazenyl]-2*H*-chromen-2-one ligand (MNB)

2.3 Synthesis of metal [Co(II), Ni(II) and Cu(II)] complexes

To prepare the complexes, a hot ethanolic solution containing 0.002 mol of ligand (MNB) was mixed with hot ethanolic solution of 0.001 mol hydrated metal chlorides (Co,Ni and Cu). The addition of the metal chlorides solution was done slowly dropwise with continuous stirring. The resulting mixture was stirred and refluxed on a water bath for 5-6 hrs at 60-70 ℃. After refluxing, the reaction mixture was cooled to room temperature. The coloured precipitate formed was then collected, washed with ethanol to remove impurities. Finally the obtained complexes were dried and stored in a desiccator. Scheme-2 represents the synthetic path of metal complexes and their proposed structure. Yield 65-73%.

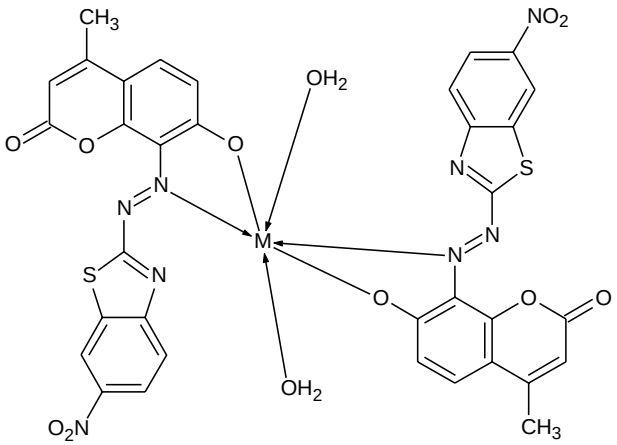

Scheme 2. Schematic representation of metal complexes

2.4 Photodegradation study

Photodegradation experiments were performed on metal complexes as photocatalysts for Methylene blue (MB) dye under UV light, utilizing natural sunlight irradiation. Initially, a solution of MB was prepared by dissolving it in 100 mL of deionized water. Subsequently, 50 mg of the metal complexes, serving as the photocatalyst, were added to the solution. The mixture was then allowed to equilibrate in darkness for a duration of 15 minutes to establish a baseline condition.Following the equilibration period, the solution was exposed to natural sunlight. At regular intervals of 15 minutes, aliquot samples were withdrawn from the solution for analysis. The degradation percentage of the dye solution was measured using a UV-Visible spectrometer.This experimental setup enables the assessment of the efficacy of the metal complexes as photocatalysts in degrading the MB dye under natural sunlight exposure. By periodically sampling the solution and analysing the degradation percentage, the kinetics of the photodegradation process can be elucidated. Additionally, the use of natural sunlight as the light source ensures a practical and environmentally friendly approach to assess the photocatalytic activity of the metal complexes [17-18].

2.5 Pharmacology

2.5.1 Antibacterial and antifungal screening

The synthesized compounds were subjected to antibacterial activity testing using a modified version of the agar well diffusion method described by standard procedure [19]. The test panel included two gram-positive bacterial strains (staphylococcus aureus and Escherichia coli) two gram-negative bacterial strains (Acetobacter sp. And Pseudomonas aeeuginosa),

and two fungal species (A.flavous and P.anomala). A standard drug was also included for comparisison.

Inoculums were prepared in sterile saline solution and adjusted to approximately 5 x 10CFU/mL. All synthesized substances were dissolved in dimethyl sulfoxide (DMSO) to create a stock solution of 10 mg/mL. Varying concentrations ranging from 100 to 500 µg were loaded into five separate wells. The employed media were Czapeks-Doxagar for fungi and nutrient agar for bacteria. As a positive control, conventional antibiotics Rifampicin (5 µ/Disc), Bacitracin (10 µ/Disc), and Fluconazole were utilized for microorganisms, while DMSO as a negative control revealed no inhibition zone (mm) was measured after 24 hours of incubation at 28 ℃ for fungi and 37 ℃ for bacteria. The relative percentage inhibition was computed against the standard medication using the formula [20].

2.5.2 Antioxidant activities (DPPH method)

The stable DPPH radical was utilized to asses the radical-scavenging capabilities of compounds with slight modifications to the procedure [21]. A spectrometer (Shimadzu UV-1800, Kyoto, Japan) was used to measure absorbance at 517 nm against a blank (without compound and standard). The results were expressed in IC50 values. In brief, 3 mL of appropriately diluted compounds in methanol and 0.5 mL of DPPH (500 µM) were combined. The reaction mixture was subsequently incubated in darkness for 45 minutes at room temperature. Butylated hydroxytoluene (BHT) was employed as a reference antioxidant.

2.5.3Molecular docking studies

The molecular docking studies had been carried out using HEX 8.2 software in order to comprehend the binding interaction modes of the synthesized compounds in comparison to the compare cytotoxicity effect [22-23]. Using Chem Sketch and Chem3D Ultra the potential structures for the complexes docking experiments were created. The RCSB Protein Data Bank was searched for the protein Epidermal growth factor receptor (EGFR) tyrosine kinase in PDB format (PDB ID: 1M17). The docking calculation with correlationform, Fourier Transform, FFT steric experiment, FFT final search, and MM refinement had all used the default settings. A stronger binding interaction between the drug and the receptor, which results in the inhibition of receptor activity, is indicated by a higher negative E-total value.

3. Results and discussion

3.1Chemistry

It has been observed that the ligand and its metal complexes exhibit stability under atmospheric conditions when dissolved in polar solvents such as ethanol, methanol, DMF, DMSO, and chloroform. Table 1 provides analytical and physical data for MNB and its metal complexes, indicating a consistent metal-to-ligand ratio of 1:2 across all complexes. Molar conductivity values for the complexes were determined at room temperature in a 0.001 M concentration of DMF solution. It was noted that the conductivity values for the metal complexes fell within the range of 23 to 27 cm^2mol^{-1}, suggesting non-electrolytic behaviour.

Table 1. Physical properties and analytical data of the MNB and their complexes

Compounds and color	Mol.wt	Yield (%)	CHN Analysis Found (Calculated %)				Molar conductance ($ohm^{-1}cm^2mol^{-1}$)	M.P. (℃)
			M	C	H	N		
Ligand (MNB)	382.35	69	-	53.40 (52.66)	2.64 (2.44)	14.65 (13.67)		170
$[Co(MNB)_2(OH_2)_2]$	857.64	70	8.30 (8.10)	47.61 (46.89)	2.59 (2.45)	13.07 (12.88)	23	260
$[Ni(MNB)_2(OH_2)_2]$	862.26	67	8.28 (8.40)	47.63 (46.88)	2.59 (2.35)	13.07 (13.22)	25	265
$[Cu(MNB)_2(OH_2)_2]$	857.40	73	8.10 (8.35)	47.36 (47.58)	2.57 (2.25)	13.00 (12.75)	27	268

3.2 ^{1}H and ^{13}C NMR spectral studies

The NMR spectra of the azo-dye ligand were obtained using DMSO-d6 as the solvent at room temperature, and TMS was used as an internal standard. Within the spectra, the ligand MNB exhibited signals a singlet at 10.53 ppm attributed to the -OH protons (s, 1H, OH) of the coumarine ring, peaks ranging from 6.20 to 7.5 ppm representing the aromatic protons of the ligand (m, Ar-6H) and a singlet at 2.5 ppm corresponding to the $-CH_3$ group (s, 3H, CH_3) of the coumarine ring.

The ^{13}C NMR spectrum of the MNB ligand exhibits carbon atoms distributed across aa range of chemical shifts from 21.2 to 166.9 ppm. Notably, the C=O group of the ligand resonates as a singular peak at 166.9 ppm, which another distinct signal appears at 160.9 ppm, attributed to the aromatic C=N within the coumarine ring. Additionally, the carbon atom proximal to the diazo group (=C-N) displays resonance at 159.04 ppm. Furthermore, the (C-OH) moiety

of the benzene ring manifests a singular peak at 161.64 ppm. Within the 102.63 to 132.03 ppm region corresponds to resonance of aromatic carbons, while the signal at 21.2 ppm arises from the methyl carbon (CH_3-C) of the coumarin ring. Figure are given in Fig 2.

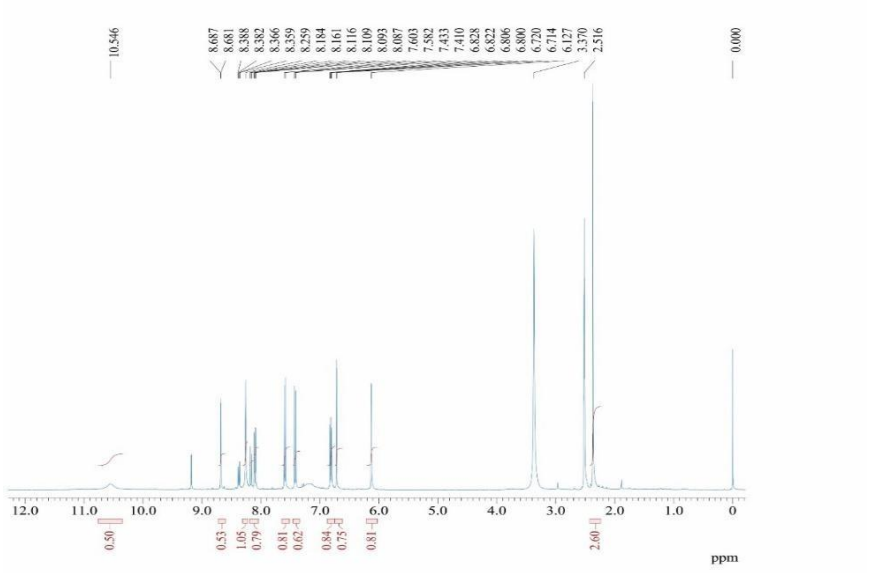

Figure 1. ^{1}H NMR spectrum of MNB

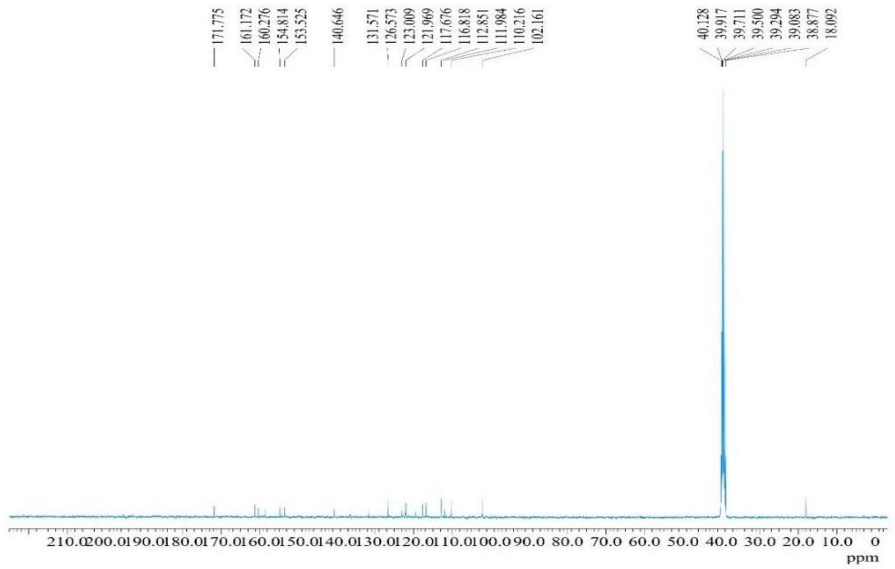

Figure 2. ^{13}C NMR spectrum of MNB

3.3 Mass spectral studies

The mass spectrum of the ligand (MNB) a distinct molecular ion peak at m/z 382.53 (cal 381.40), corresponding to (M+ 1), suggesting the proposed molecular formula weight of the ligand is showed in Fig 2. The molecular ion peaks observed for the Co(II), Ni(II) and Cu(II)complexes are at m/z 857.64 (cal 856.33), 862.26 (cal 861.62) and 857.40 (cal 856.50) respectively, indicating a stoichiometric ratio of 1:2 (M:L). These observed molecular masses align with the proposed molecular structures of the prepared complexes, confirming their consistency. The mass spectra of the metal complexes are given in Figures 4,5 and 6.

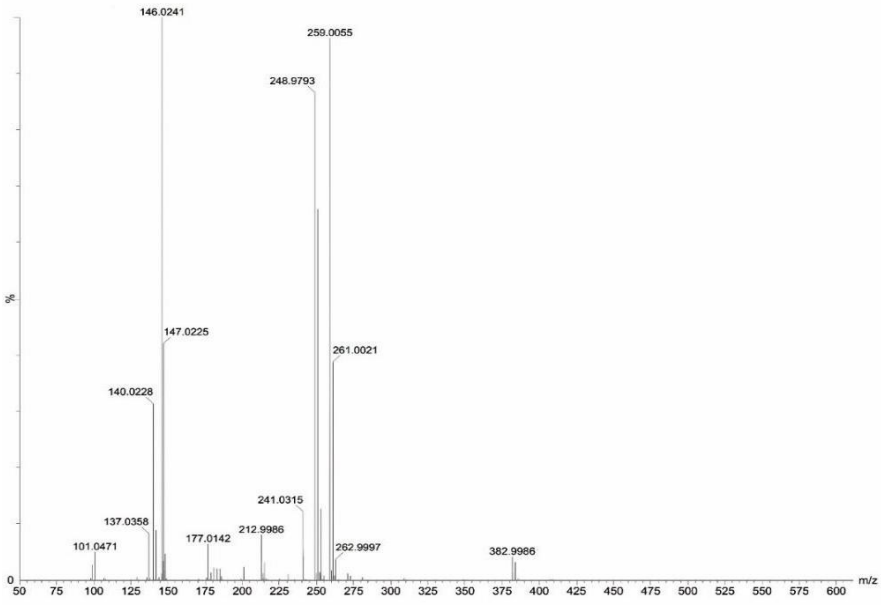

Figure 3. Mass spectrum of MNB

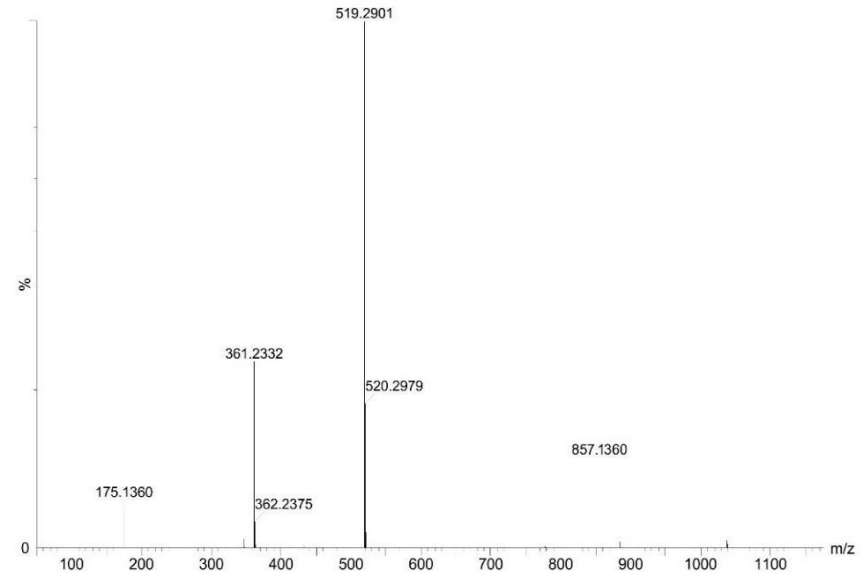

Figure 4. Mass spectrum of [Co(MNB)$_2$(OH2)$_2$]

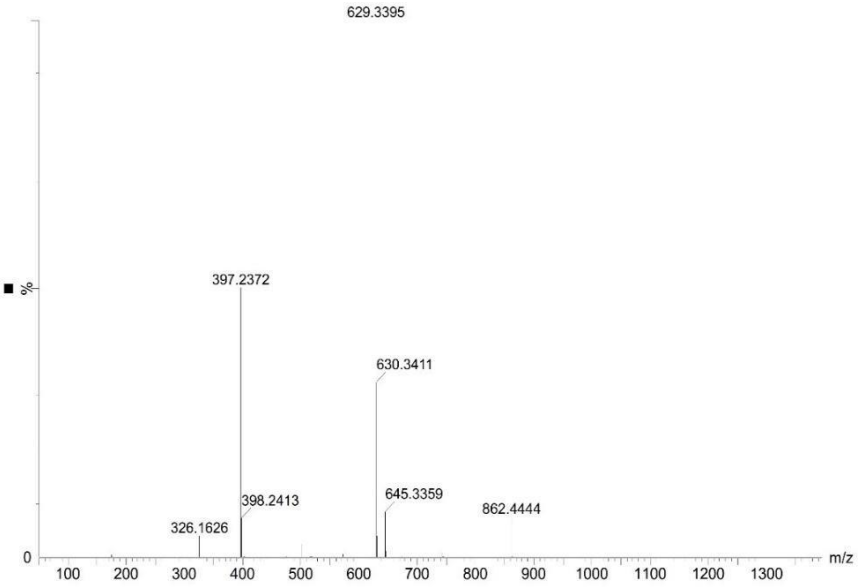

Figure 5. Mass spectrum of [Ni(MNB)$_2$(OH2)$_2$]

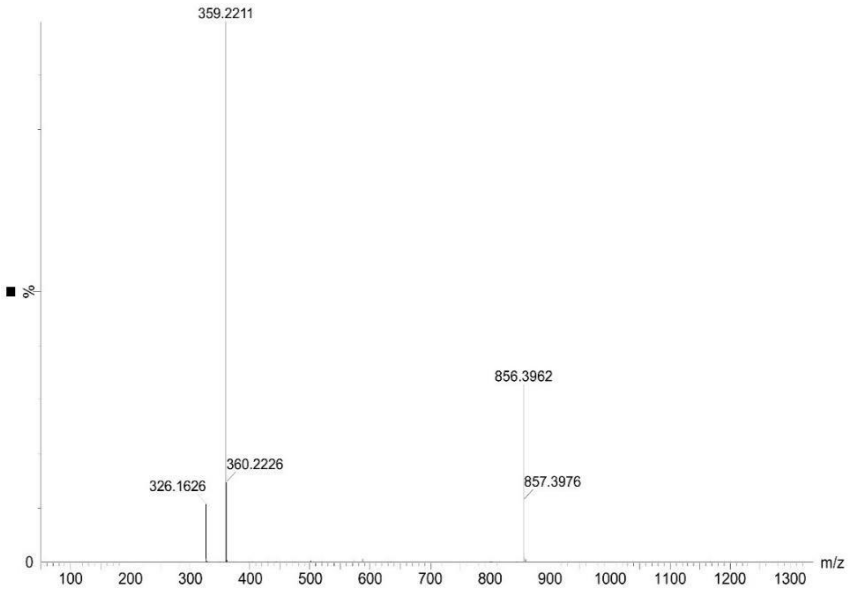

Figure 6. Mass spectrum of [Cu(MNB)$_2$(OH2)$_2$]

3.4IR spectral studies

The IR spectra analysis of an azo-dye ligand and its metal complexes, conducted using KBr pellets in the range of 4000-350 cm-1, reveals significant insights into their coordination behaviour. In the ligand spectrum, a distinctive absorption band at 3150 cm-1 is attributed to -OH stretching vibration, which notably shifts to higher frequencies in all complexes, indicating the involvement of the hydroxyl group in complexation [24]. Additionally, a sharp band at 1360 cm-1 corresponding to the N=N azo group is observed in the ligand spectrum, with a consistent shift to higher frequencies in complexes, suggesting azo group participation in complex formation. Notably, intense sharp peaks at 1130 cm-1 and 1690 cm-1, attributed to C=N and C=O stretching vibrations, respectively, remain unaltered in the metal-coordinated compounds, suggesting that these functional groups are not involved in complexation. However, the emergence of new bands in IR spectra of metal-coordinated compounds, particularly in the 582-590 cm-1 region indicative of metal ion coordination with oxygen, and in the 432-450 cm-1 region suggesting metal ion coordination with nitrogen, provide compelling evidence for the complexation of the azo-dye ligand with metal ions. These spectral shifts and the appearance of new bands offer valuable insights into the specific functional groups involved in the coordination process.

Table 2. FT-IR spectral data (cm-1) of MNB and its metal complex

Compounds	*V*(OH)	*V*(C=N)	*V*(N=N)	*V*(C=O)	*V*(M-O)	*V*(M-N)
MNB	3150	1135	1366	1690	-	-
[Co(MNB)$_2$(OH2)$_2$]	3400	1137	1380	1685	450	590

$[Ni(MNB)_2(OH2)_2]$	3385	1138	1381	1690	432	585
$[Cu(MNB)_2(OH2)_2]$	3380	1136	1381	1690	445	582

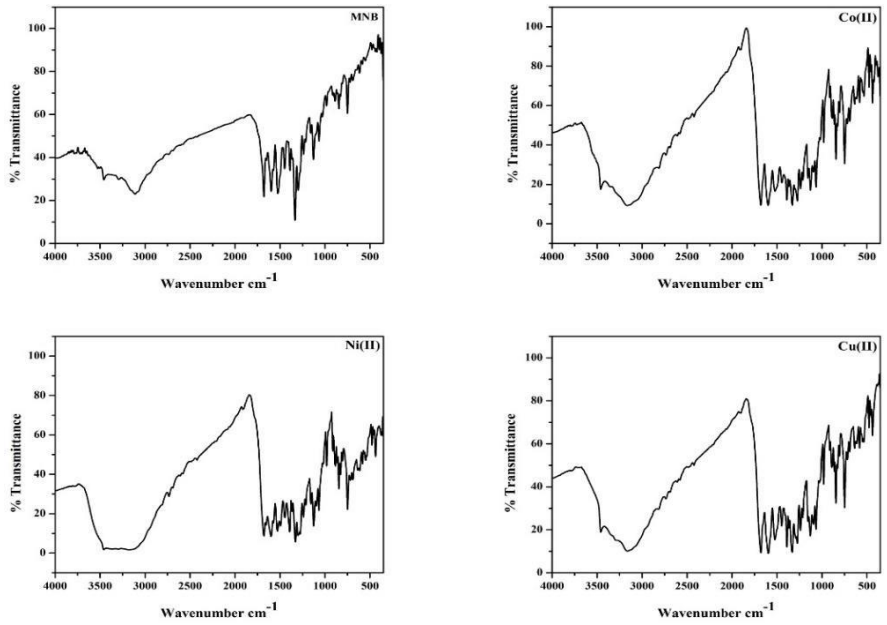

Figure 7. FT-IR spectra of MNB and their metal complexes

3.5Electronic spectra and magnetic moment studies

The electronic spectra of the synthesized azo-dye ligand and its metal complexes are displayed in Fig.8. and the values are presented in Table 3. Electronic spectra were recorded for all compounds in DMSO solution within the wavelength range of 200-900 nm. The electronic spectrum of the Co(II) complex, exhibiting a light green colour, displayed a broad peak at 21,739, 16,393 and 14,925 cm-1 attributed to $^4T_{1g}(F)\rightarrow{}^4T_{2g}(F)$ (v_1), $^4T_{1g}(F)\rightarrow{}^4A_{2g}(F)$ (v_2) and $^4T_{1g}(F)\rightarrow{}^4T_{1g}(F)$ (v_3) transitions respectively. The observed magnetic moment value of 3.6 B.M suggests an octahedral geometry for this complex. Subsequently, The Ni(II) complex, appearing brown in colour, exhibited two absorption bands at 18,181, 16,129 and 13,157 cm-1.$^3A_{2g}(F)\rightarrow{}^3T_{2g}(F)$ (v_1) and the second transition $^3A_{2g}(F)\rightarrow{}^3T_{1g}(F)$ (v_2) and third ascribed to $^3A_{2g}(F)\rightarrow{}^3T_{1g}(F)$ (v_3). Inaddition the observed magnetic moment value 2.7 BM indicate octahedral geometry.around the Nickel complex. A broad band with a maximum at 11,112cm-1 due to $^2E_g(F)\rightarrow{}^2T_{2g}(F)$ (v_1) transition for intense pale green colored Cu(II) and having magnetic moment value of 1.78 B.M for distorted octahedral geometry [25].

Table 3. Electronic absorption spectral bands of metal complexes

Compounds	**λ (nm)**	Transitions cm-1	Magnetic Moment

MNB	340	29,411	-
$[Co(MNB)_2(OH2)_2]$	460 610 670	21,739 16,393 14,925	3.6
$[Ni(MNB)_2(OH2)_2]$	550 620 760	18,181 16,129 13,157	2.7
$[Cu(MNB)_2(OH2)_2]$	900	11,112	1.78

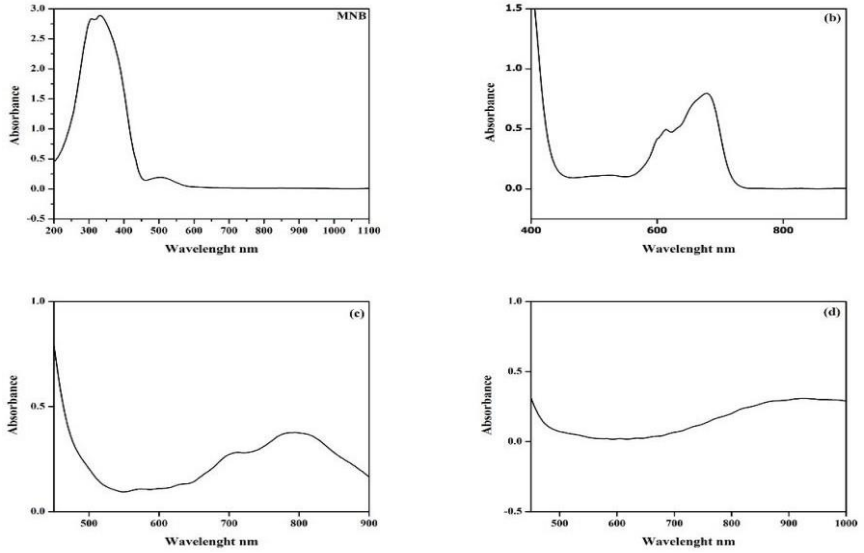

Figure 8. Electronic spectra of MNB and their metal complexes.

3.6X-ray diffraction studies

The powder X-ray diffraction (XRD) patterns of the synthesized metal complexes were recorded in the 20-80º 2Ɵ range. The diffractograms are presented in figures 9. The diffraction data, including peak angles (2Ɵ), relative intensities (%) and interplanar spacing (d) are summarized in tables 4a, 4b and 4c. The sharp peaks observed in the XRD patterns indicate the crystalline nature of the metal complexes. The average crystallite sizes of the complexes were calculated using the scherrers formula. The results revealed that the crystallite sizes of the Co(II). Ni(II) and Cu(II) complexes are within the nanometer range. These XRD analyses provide valuable insights into the structural properties and crystallinity of the synthesized metal complexes [26-27], The crystallite sizes of the complexes, which are 19.20, 7.89 and 20.22 nm, respectively indicate that the complexes are in a nanocrystalline phase.

Table 4a. Powder XRD spectral data of $[Co(MNB)_2(OH2)_2]$

Peak No.	**2θ**	**θ (degree)**	**θ (radian)**	**Sinθ**	**hkl**	**D**		**a in Å**
						Cal	**Obs**	
1	26.235	13.179	0.2245	0.2178	1 1 1	2.85	2.80	4.45
2	30.717	15.358	0.2617	0.2587	2 0 0	2.50	2.40	4.45
3	44.945	22.457	0.3839	0.3745	2 2 0	2.10	2.05	4.45
4	52.687	26.347	0.4537	0.4478	3 1 1	1.86	1.80	4.45
5	65.678	32.567	0.5585	0.5489	2 2 2	1.50	1.45	4.45
6	72.789	36.347	0.6283	0.6166	4 0 0	1.38	1.35	4.45
7	75.876	37.690	0.6457	0.6378	3 3 1	1.20	1.15	4.45
8	80.432	40.232	0.6981	0.6855	0 2 4	1.15	1.10	4.45
9	89.032	44.543	0.7679	0.7579	4 2 2	1.11	1.05	4.45

Table 4b. Powder XRD spectral data of [Ni(MNB)$_2$(OH2)$_2$]

Peak No.	**2θ**	**θ (degree)**	**θ (radian)**	**Sinθ**	**hkl**	**D**		**a in Å**
						Cal	**Obs**	
1	18.862	9.434	0.1570	0.1476	1 0 0	3.20	3.15	3.71
2	23.644	11.675	0.1919	0.1889	1 0 1	2.80	2.75	3.71
3	33.544	15.543	0.2629	0.2578	1 1 0	2.50	2.40	3.71
4	40.308	20.156	0.3490	0.3367	1 0 2	2.10	2.00	3.71
5	43.897	21.987	0.3665	0.3477	2 0 0	1.58	1.50	3.71
6	57.907	27.987	0.4712	0.4632	2 2 0	1.22	1.11	3.71

Table 4c. Powder XRD spectral data of [Cu(MNB)$_2$(OH2)$_2$]

Peak No.	**2θ**	**θ (degree)**	**θ (radian)**	**Sinθ**	**hkl**	**D**		**a in Å**
						Cal	**Obs**	
1	26.443	13.221	0.2268	0.2136	1 1 1	3.50	3.45	4.43
2	44.345	22.245	0.3839	0.3632	2 2 0	3.10	2.98	4.43
3	53.987	26.876	0.4537	0.4423	3 1 1	2.55	2.39	4.43
4	64.132	32.213	0.5585	0.5309	4 0 0	2.10	1.90	4.43
5	72.931	36.670	0.6283	0.6190	3 3 1	1.45	1.38	4.43
6	84.029	42.123	0.7330	0.7223	4 2 2	1.11	1.07	4.43

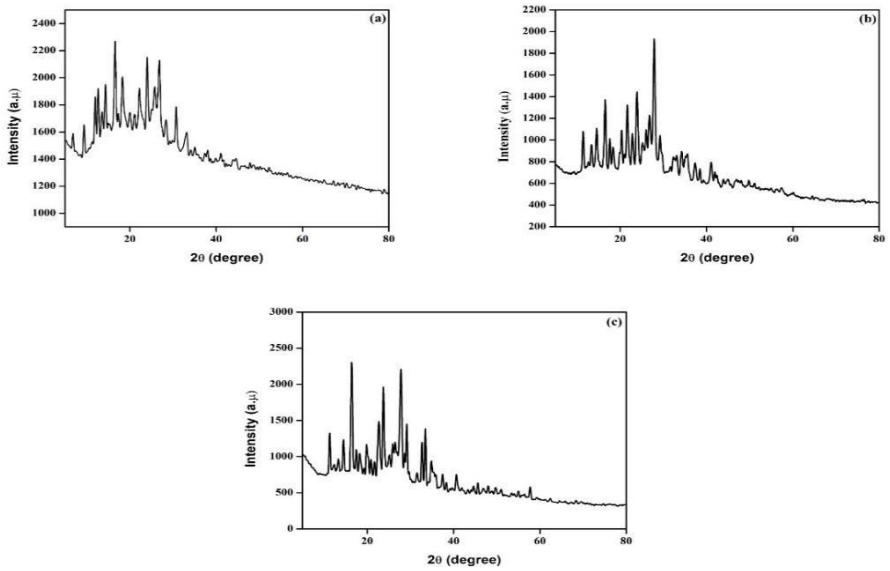

Figure 9. Powder XRD pattern of (a) [Co(MNB)$_2$(OH2)$_2$] (b) [Ni(MNB)$_2$(OH2)$_2$](c) [Cu(MNB)$_2$(OH2)$_2$]

3.7 Scanning Electron Microscopy (SEM) Analysis

SEM was employed to meticulously examine the surface characteristics of the azo-azomethine ligand and its metal complexes. Figure 10 presents the SEM images of the investigated compounds. The MNB ligand exhibited a cotton structure, while the metal complexes displayed distinct surface morphologies. Notably, [Co(MNB)$_2$(OH2)$_2$] exhibited an prismitics like structure with layered topology. In contrast, [Ni(MNB)$_2$(OH2)$_2$] and [Cu(MNB)$_2$(OH2)$_2$] revealed granular and threads like structures respectively.

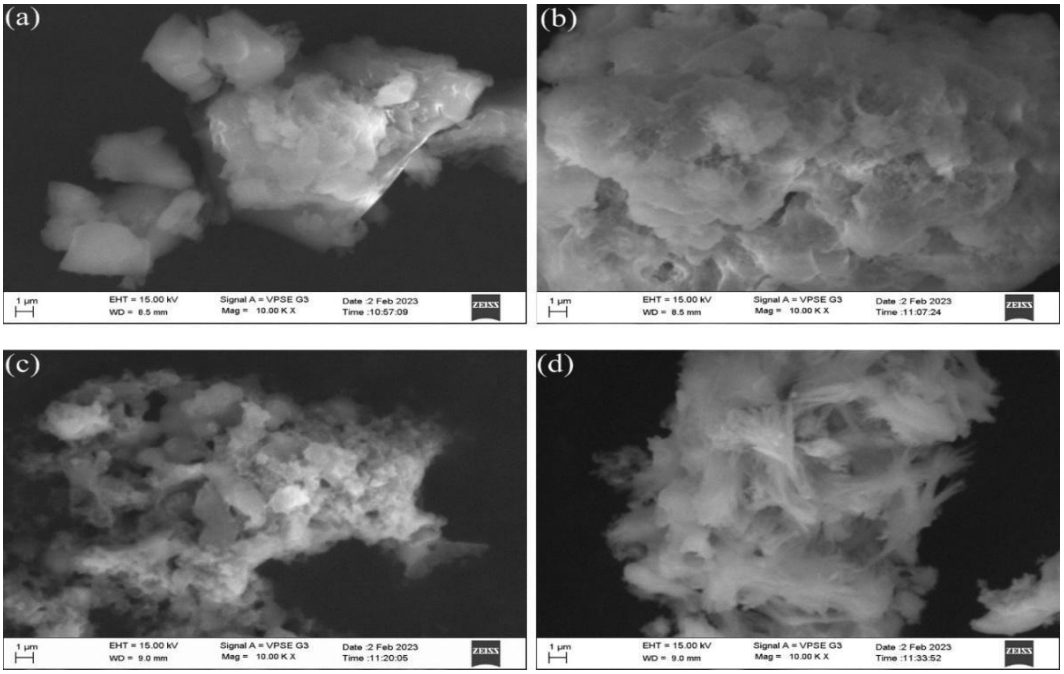

Figure 10. SEM images of (a) $[Co(MNB)_2(OH2)_2]$ (b) $[Ni(MNB)_2(OH2)_2]$(c) $[Cu(MNB)_2(OH2)_2]$

4. Photodegradation study

The photodegradation ability of synthesized metal complexes, such as Co(II), Ni(II) and Cu(II) was assessed through irradiation under natural sunlight. The degradation of MB dye was measured at wavelengths of 566.78, 570.33 and 565.98 nm for Co(II), Ni(II) and Cu(II) complexes respectively. As the irradiation time increased a decrease in MB absorbance was observed in the presence of the metal complexes. UV Visible spectra were recorded at regular time intervals of 15 minutes over a degradation time ranging from 0 to 105 minutes. Analysis of the absorbance data revealed degradation percentages of 83%, 64% and 61% for Co(II), Ni(II) and Cu(II) complexes, respectively. These results indicate that Co(II) complex exhibit superior photodegradation efficiency compared to the Ni(II) and Cu(II) complexes for MB dye.

The photodegradation percentage was calculated by using following formula [28-29].

$$\text{Percentage of degradation} = \frac{C0-Ct}{C0} \times 100$$

Where C0 represents the initial absorbance of the dye solution and Ct represents the absorbance of the dye solution in the presence of the photocatalysts Co(II), Ni(II) and Cu(II) complexes at specific time intervals.

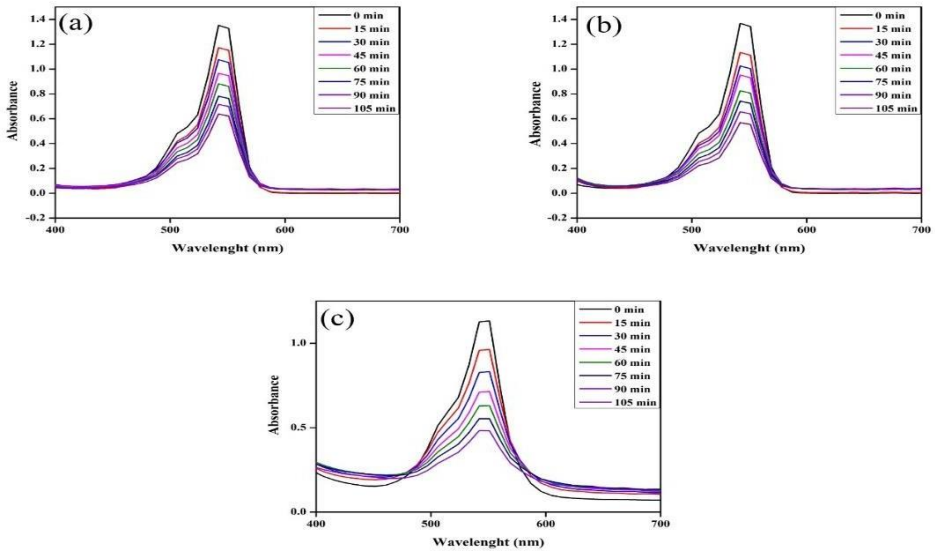

Figure 11. Photodegradation of MB dye by (a) [Co(MNB)$_2$(OH2)$_2$] (b) [Ni(MNB)$_2$(OH2)$_2$](c) [Cu(MNB)$_2$(OH2)$_2$]

5 Results and Discussion of Biological activities

5.1 Antimicrobial activity

The antimicrobial characteristics of the MNB and its metal complexes were assessed in vitro against various bacterial and fungal species. The results of these activities are presented in table 5 and graphically illustrated in figures 12 and 13. Owing to chelation, which enhances lipophilicity and promotes absorption through the bacterial membrane, leading to the demise of the organisms, metal complexes exhibit superior antibacterial activity compared to ligand, as evidenced by their larger inhibition zones [31-32]. It is noteworthy that within a complex, the positive charge of the metal is partially shared with the donor atoms present in the ligand and there may be n-electron delocalization across the entire chelating space. Consequently, the metal chelates exhibit increased lipophilicity, facilitating their passage through the lipoid layer of bacterial membranes. These compounds demonstrate a higher lipophilic character, potentially explaining their enhanced antibacterial efficacy. Additional factors influencing activity include solubility, conductivity and bond length between the metal complexes and ligand. Notably, the MNB-1 and MNB-2 complexes display superior activity against bacteria and fungi, as evidenced by significant zones of inhibition values.

Table 5. Antimicrobial activity of MNB and its metal complexes (inhibition zone in mm)

Compound	Antibacterial activity				Antifungal activity			
	Staphylococcus Aureus		Escherichia coli		A.flavous		P.anomala	
	100	200	100	200	100	200	100	200
MNB	10±1.15	11±1.52	11±1.52	12±0.57	10±1.18	13±1.43	11±0.97	15±1.18
MNB-1	19±1.52	20±0.57	21±1.52	23±0.57	24±1.43	26±0.97	26±0.87	28±1.18
MNB-2	18±1.73	20±0.57	20±1.52	21±1.15	22±0.97	23±1.43	25±0.97	27±0.97
MNB-3	13±0.57	15±0.57	15±1.73	17±0.57	16±1.18	18±0.87	19±1.43	20±1.18
Kanamycin	21.661 ± 0.57	25.78±0.57	25.30± 0.57	28.66±0.57	-	-	-	-
Fluconazole	-	-	-	-	30±1.18	34±1.43	32±1.18	36±0.97

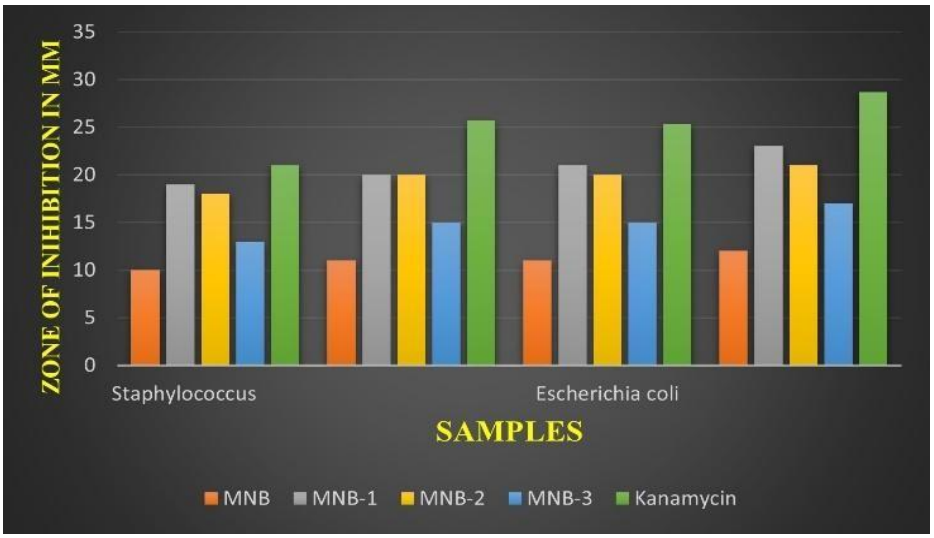

Figure 12. Antibacterial activity of MNB and its metal complexes

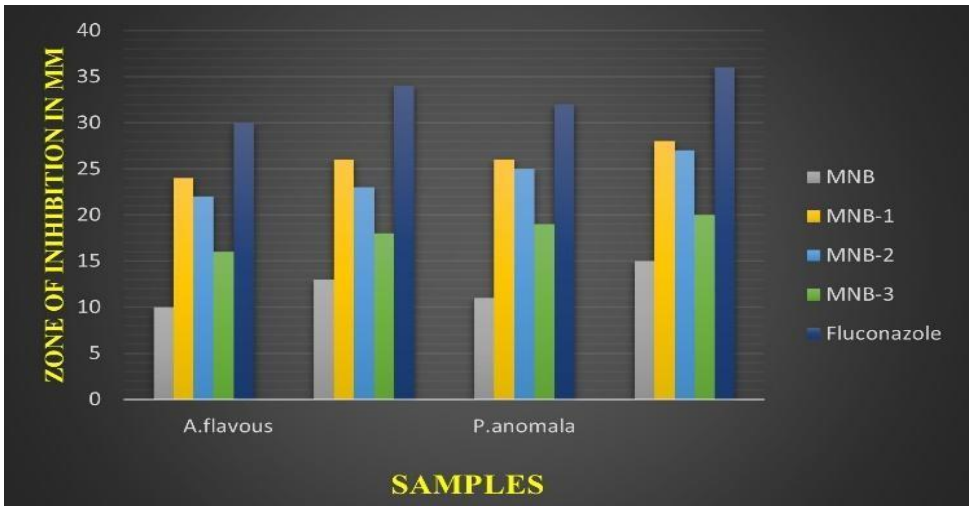

Figure 13. Antifungal activity of MNB and its metal complexes

5.2 Antioxidant Efficacy

The antioxidant capabilities of the synthesized ligand and its corresponding metal complexes were meticulously evaluated in accordance with the established methodology outlined in the methodology section. The detailed results are presented in Table 6, while a comparative analysis is provided in Figure 14. Notably, the Ni(II) and Cu(II) complexes demonstrated significantly enhanced DPPH scavenging activity across varying concentration ranging from 50 to 250 pg/mL.Furthermore, the antioxidant activity evaluation through the iron chelating assay revealed that the Ni(II) and Cu(II) complexes exhibited exceptional antioxidant efficacy in comparison to Co(II) and the uncoordinated ligand. However, it is crucial to acknowledge that the antioxidant activity of both the ligand and its complexes was relatively lower when compared BHT (Butylated hydroxytoluene) served as the standard for antioxidant activity assessment using the iron chelating assay [33-34].

Table 6. Antioxidant activity of MNB and its metal complexes

Compound	% of Scavenging activity (Concentration in µg/mL)				
	20	40	60	80	100
MNB	12±0.14	25±0.13	36±1.09	59±0.15	80±2.9
MNB-1	16±0.16	30±0.16	49±1.15	67±0.80	89±0.14
MNB-2	20±0.10	42±0.14	65±0.16	79±0.70	97±0.33
MNB-3	22±0.22	54±0.01	73±0.14	85±0.78	102±0.01
Std(BHT)	28±0.18	61±0.24	85±0.60	99±0.14	115±0.08

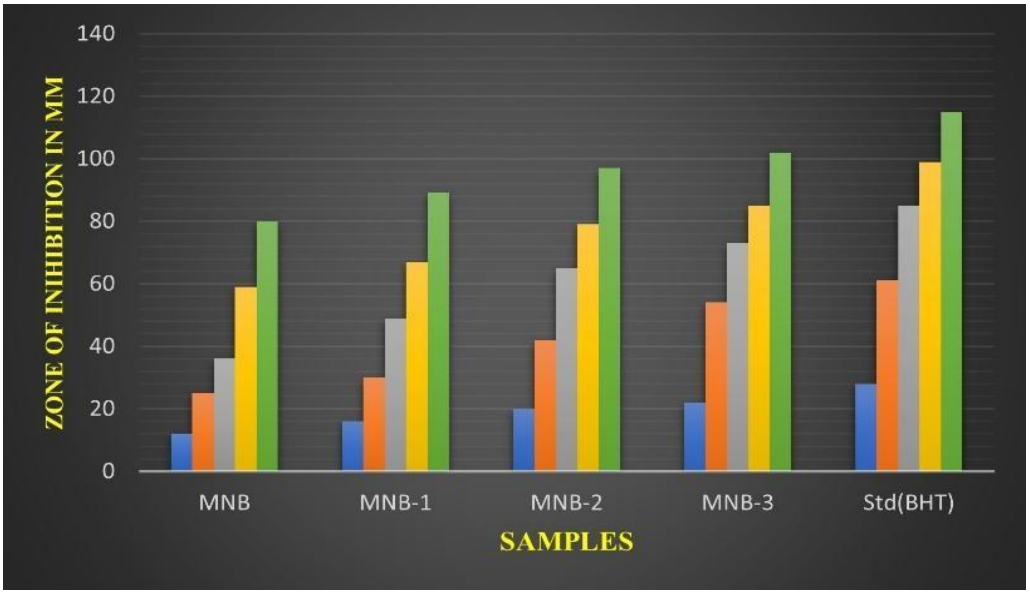

Figure 14. Antioxidant activity of MNB and its metal complexes

5.3 Docking studies

The molecular docking study correspondence with cytotoxic active receptor PDB id: 3F8G were taken and the results obtained in table 7 and their 3D interactions displayed in Fig.15. The synthesized PDP and their metal complexes exhibited binding with several amino acids in the enzyme sites [33], all the compounds displayed good binding affinity. The $[Co(MNB)_2(OH2)_2]$, $[Ni(MNB)_2(OH2)_2]$and $[Cu(MNB)_2(OH2)_2]$complexes gives highest binding interaction of -259.77, -257.46 and -268.31 $kcal^{-1}$mol respectively. Among the synthesized complexes the $[Co(MNB)_2(OH2)_2]$show highest binding affinity because they suggest a more stable and favourable interaction between the ligand and their metal complexes with receptor.

Table7. Binding energy values of MNB and their metal complexes

Compounds	Receptor	E (kcal mol^{-1}) PDB ID: 3F8G
MNB	2A91	-158.25
MNB-1	2A91	-259.77
MNB-2	2A91	-257.46
MNB-3	2A91	-268.31
Actinoin (STD)	2A91	-235.87

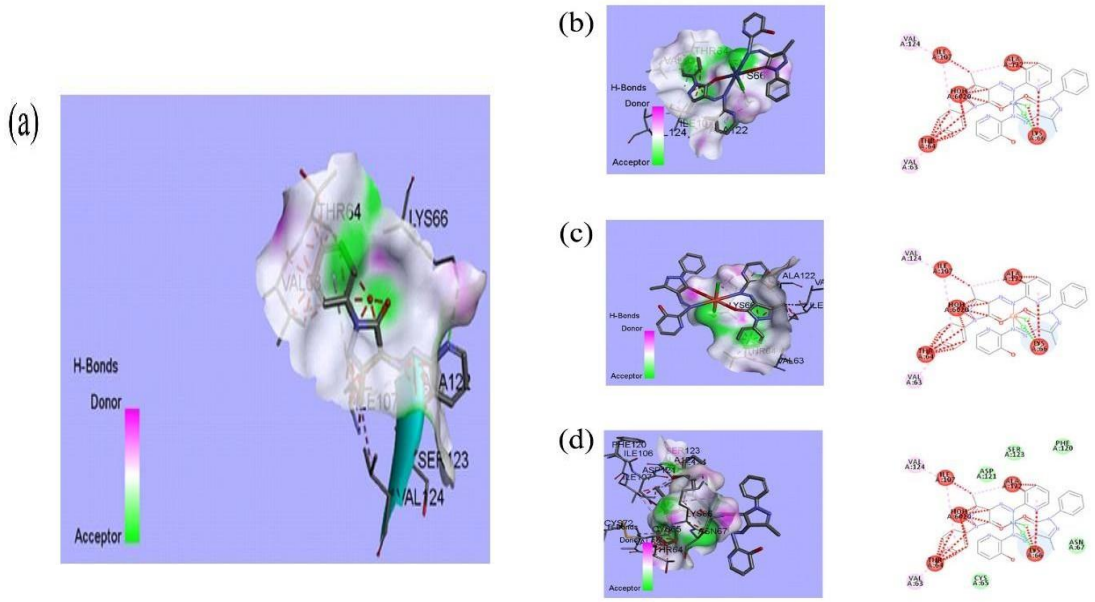

Figure 15. Molecular docking of (a) PDP (b) [Co(MNB)$_2$(OH2)$_2$] (c) [Ni(MNB)$_2$(OH2)$_2$] (d) [Cu(MNB)$_2$(OH2)$_2$]

Conclusion

In this study, a novel ligand 7-hydroxy-4-methyl-8-[(*E*)-(6-nitro-1,3-benzothiazol-2-yl)diazenyl]-2*H*-chromen-2-one ligand (MNB)was synthesized to produce biologically active Co, Ni and Cu complex. These complexes were evaluated using a various of physicochemical and spectral approaches. Using a variety of analytical methods, we were able to determine the structure of MNB and its metallic compounds. The synthetic procedure employed in this investigation revealed the formation of complexes with a metal to ligand molar ratio 1:2. According to molar conductance data, the complexes exhibited non electrolytic behaviour. Based on UV-Vis and magnetic Susceptibility data, the complexes adopt a square planar geometry.The photocatalytic activity of the synthesized complexes was evaluated using MB dye, with theCo(II) complex demonstrating a superior degradation efficiency compared to other metal complexes. Furthermore, the antimicrobial of the uncoordinated ligand and its metal complexes were investigated. The results revealed that the MNB-1 and MNB-2 complexes exhibited enhanced biological activity compared to the ligand itself.

Acknowledgement

The authors thanks to Sahyadri Science College Kuvempu University, University of Mangaluru, for providing spectral facilities. Authors are also thankfull to Cheliyan biotech solutions nanjanagudu for biological study.

Declaration of competing Interest

The authors declare that they have no competing financial interests or personal relationships that would have appeared to influence the work reported in this paper.

Reference

1. N. Ranjitha, G. Krishanamurthy, M.N. Manjunath, H.S. Bhojya Naik, Malathesh Pari, N,K. Vasanthkumarnaik, J. Lakshmikantha, K. Pradeep, Electrochemical determination of glucose and H_2O_2 using Co(II, Ni(II), Cu(II) complexes of novel 2-(1,3-benzothiazol-2-ylamino)-N-(5-chloro-2-hydroxyphenyl)acetamide:Synthesis, structural characterisation, antimicrobial, anticancer activity and docking studies. J. Mol. Struct. 2023,1274, 134483, https://doi.org/10.1016/j.molstruc.2022.134483
2. N. Venugopal, G. Krishnamurthy, H.S. Bhojya Naik, P. Muruli Krishna,Synthesis, spectral characterization and biological studies of Cu (II), Co (II) and Ni (II) complexes of azo dye ligand containing 4–amino antipyrine moiety. J. Mol. Struct, 2019,1183, 37-51,https://doi.org/10.1016/j.molstruc.2019.01.031
3. N. Sunil Kumar, G. Krishnamurthy, D. Yadav Bodke, Vikas Malojirao, T.R. Ravikumar Naik, ShivanandaKandagalla, B.T. Prabhakar, Synthesis, characterization and tumor inhibitory activity of a novel Pd(II) complex derived from methanethiol-bridged (2-((1*H*-benzo[*d*]imidazol-2-yl)methylthio)-1*H*-benzo[*d*]imidazol-6-yl)(phenyl)methanone. New J Chem, 43, 2019, 790-806,https://doi.org/10.1039/C8NJ03057J
4. N. Sunil Kumar, G. Krishnamurthy, Madhusudanasomegowda, Maltesh Pari, T. R. Ravikumar Naik, K.S. Jithendra Kumar, Satish Naik.; ShivanandaKandagalla.; Nagaraja Naik.; Synthesis, characterization, electrochemistry, biological and molecular docking studies of the novel Co(II), Ni(II) and Cu(II) complexes derived from methanethiol bridged (2-((1H-benzo[d]imidazol-2-yl)methylthio)-1H-benzo[d]imidazol-6-yl)(phenyl)methanone. J. Mol. Struct, 2020, 128586, 1220,

https://doi.org/10.1016/j.molstruc.2020.128586

5. Xuhua, Dong. Siqi, Xie. Jingyang, Zhu. Haiquan, Liu Yong, Zhao., Tianjun, Ni, Long, Wu, Yongheng, Zhu. Mesoporous CoOx/C Nanocomposites Functionalized Electrochemical Sensor for Rapid and Continuous Detection of Nitrite. *Coatings* 2021, *11*, 596.
https://doi.org/10.3390/coatings11050596
6. N. Venugopal, G. Krishnamurthy, H.S. Bhojya Naik, M. Giridhar, Novel bioactive azo-azomethine based Cu (II), Co (II) and Ni(II) complexes, structural determination and biological activity. J. Mol. Struct, 2019, 1191, 85-94,
https://doi.org/10.1016/j.molstruc.2019.04.022
7. L. Cottet, C.A.P Almeida, N. Naidek, M.F. Viante, M.C. Lopes, N.A. Debacher, Adsorption characteristics of montmorillonite clay modified with iron oxide with respect to methylene blue in aqueous media. Appl.Clay. Scie, 2014, 95, 25-31,
https://doi.org/10.1016/j.clay.2014.03.023
8. K. Khalid AL-Adilee, K. Ahmed Abass, M. Taher, Synthesis of some transition metal complexes with new heterocyclic thiazolyl azo dye and their uses as sensitizers in photo reactions. J. Mol. Struct, 2016, 1108, 378-397,
https://doi.org/10.1016/j.molstruc.2015.11.038
9. Zabiulla, Salma Kouser, Mahima Joythi. A. Bushra Begum, M.S. Asha, Fares Hezam Al-Ostoot. D.P. Lakshmeesha, Ramith Ramu, Shaukath Ara Khanum,Molecular docking, synthesis and antimicrobial evaluation of metal complexes with Schiff base. Results in Chem, 2018, 5, 100650, https://doi.org/10.1016/j.rechem.2022.100650
10. A.G. Prashantha, R.A. Shoukat Ali, J. Keshavayya, Synthesis, spectral characterization, DFT studies and antimicrobial activities of amino-methylbenzoic acid based azo dyes. InorG.CheM.Commun. 2021, 127, 108392, https://doi.org/10.1016/j.inoche.2020.108392
11. May Juda Kareema, Abbas Ali Salih Al-Hamdani, Young Gun Ko, Wail Al Zoubi Saad, G. Mohammed, Synthesis, characterization, and determination antioxidant activities for new Schiff base complexes derived from 2-(1H-indol-3-yl)-ethylamine and metal ion complexes. *J.Mol.Struct.* 2021, *1231*, 129669, https://doi.org/10.1016/j.molstruc.2020.129669

12. H.R. Zare, N. Nasirizadeh, M. Mazloum Ardakani, Electrochemical properties of a tetrabromo-*p*-benzoquinone modified carbon paste electrode. Application to the simultaneous determination of ascorbic acid, dopamine and uric acid. JEAC, 2005, 577(1), 25-33, https://doi.org/10.1016/j.jelechem.2004.11.010

13. P. Manivel, M. Dhakshnamoorthy, A. Balamurugan, N. Ponpandian, D. Mangalaraj, C. Viswanathan, Conducting polyaniline-graphene oxide fibrous nanocomposites: preparation, characterization and simultaneous electrochemical detection of ascorbic acid, dopamine and uric acid. RSC Advances 2013, 3(34), 14428-14437,

14. N. Manjunatha, A. Shambulinga, D. Imdadulla, C.P. KeshavanandaPrabhu, K.S. Lokesh, Chemisorbed palladium phthalocyanine for simultaneous determination of biomolecules. Microchem, 2018, 143, 82, https://doi.org/10.1016/j.microc.2018.07.039

15. Malathesh Pari, K.R. Venugopala Reddy, Fasiulla, K.B. Chandrakala, Amperometricdetermination of dopamine based on an interface platform comprising tetra-substituted Zn^{2+} phthalocyanine film layer with embedment of reduced graphene oxide. Sens, 2020, Vol.316, 112377,https://doi.org/10.1016/j.sna.2020.112377

16. P. Manivel, M. Dhakshnamoorthy, A. Balamurugan, N. Ponpandian, D. Mangalaraj, C. Viswanathan, Conducting polyaniline-graphene oxide fibrous nanocomposites: preparation, characterization and simultaneous electrochemical detection of ascorbic acid, dopamine and uric acid. RSC Adv. 3(34), 14428-14437, (2013)https://doi.org/10.1039/C3RA42322K

17. Ana Claudia, Jefferson Bettini, Manoella da Silva Cavalcante, Mariane Peres Pereira, Carlos Cesar BofBufon, MuriloSanthiago, Mathias Strauss, Boosting Electrical Conductivity of Sugarcane Cellulose and Lignin Biocarbons through Annealing under Isopropanol Vapor. ACS Sustain. Chem. Eng. 8(18),7002-7010, (2020).https://doi.org/10.1021/acssuschemeng.0c00320

18. S Nagashree, CS Karthik, BL Sudarshan, L Mallesha, HP Spoorthy, KR Sanjay, P Mallu. In vitro antimicrobial activity of new 2-amino-4-chloropyridine derivatives: A structure-activity relationship study. J. Pharm. Res. 9 (8), 509-516, (2015).ISSN: 0974-6943

19. R. Monica Loizzo, Rosa Tundis, Marco Bonesi, FedericMenichini, Vincenzo Mastellone, Radical scavenging, antioxidant and metal chelating activities of *Annona cherimola* Mill. (cherimoya) peel and pulp in relation to their total phenolic and total flavonoid contents. J Food Compost Anal. 25(2), 179-184, (2012).https://doi.org/10.1016/j.jfca.2011.09.002

20. Sudarshan BikikallahalliLakshmegowda, Sanjay Konasur Rajesh, Hemanth Kumar Kandikattu, IlaiyarajaNallamuthu, Farhath Khanum, In Vitro and In Vivo Studies on Hexane Fraction of Nitzschiapalea, a Freshwater Diatom for Oxidative Damage Protective and Anti-inflammatory Response. Rev.bras.farmacogn. 30, 189-201, (2020).10.1007/s43450-020-00008-6

21. Andreea N Kiss, Wade M Danis, S Tamer Cavusgil, International entrepreneurship research

in emerging economies: A critical review and research agenda. J.Bus.Ventur. 27(2), 266

290, (2012).https://doi.org/10.1016/j.jbusvent.2011.09.004

22. MahdiehMehrpouri, Ava Safaroghli-Azar, Majid Momeny, DavoodBashash, Anti-leukemic effects of histone deacetylase (HDAC) inhibition in acute lymphoblastic leukemia (ALL) cells: Shedding light on mitigating effects of NF-κB and autophagy on panobinostat cytotoxicity. Eur. J. Pharmacol. 875, 173050, (2020).https://doi.org/10.1016/j.ejphar.2020.173050

23. T. Manjuraj, T.C.M. Yuvaraj, N.D. Jayanna, S.H. Shreedhara, M.S. Sarvajith, Spectral, DFT, molecular docking and antibacterial activity studies of Schiff base derived from furan-2-carbaldehyde and their metal(II) complexes. J. Turkish chem. Soc. 7(2), 449-462, (2020). https://doi.org/10.18596/jotcsa.467859

24. T. Manjuraj, G. Krishnamurthy, D. Yadav Bodke, H.S, Bhojya Naik, H.S. Anil Kumar, Synthesis, XRD, thermal, spectroscopic studies and biological evaluation of Co(II), Ni(II) Cu(II) metal complexes derived from 2-benzimidazole. J. Mol. Struct. 1171, 481-487, (2018). https://doi.org/10.1016/j.molstruc.2018.06.055

25. Vishnu G, Simranjeet Singh , T.S.Sunil KumarNaik, R. Viswanath [a], Pooja Bhadrecha, H S Bhojya Naik, Joginder Singh, A. Nadeem Khan, Sasan Zahmatkesh, Photodegradation of methylene blue dye using light driven photocatalyst-green cobalt doped cadmium ferrite nanoparticles as antibacterial agents, J.Clean.Prod. 404, 2023, 136977 https://doi.org/10.1016/j.jclepro.2023.136977

26. Pardeep Singh, M.C. Vishnu, KaranKumar Sharma, Anwesha Borthakur, Pratap Srivasta, D.B Pal, Dhanesh Tiwary, Pradeep Kumar Mishra, Photocatalytic degradation of AcidRed dye stuff in the presence of activated carbon-TiO_2 composite and its kineticenumeration, (JWPE), 12, 2016, 20-31, https://doi.org/10.1016/j.jwpe.2016.04.007

27. VasantakumaranaikNarayanapuraKrishnanaik, Ganganaik Krishnamurthy, MalatheshPari, Nagaraju Venugopal, NanjundaswamyRanjitha, Nagaraja Naik, Synthesis, Spectral Characterisation of Novel Azo–Dye 4((E)-(2-Hydroxy-3- Methoxy-5-((E)-Thiazol2Yldiazenyl)Benzylidene)Amino)-1,5-Dimethyl-2- Phenyl1H-Pyrazol-3(2H)-One and its Transition Metal Complexes; Differential Pulse Voltammetric Detection of Nitrite and its Biological Activities, Biointerface Res. Appl. Chem., 2023, 13, 531, doi: 10.33263/BRIAC136.531

28. Samira M. Abozeid, Eric M. Snyder, Alejandra P. Lopez, Charles Steuerwald, EricSylvester, K M. Ibrahim, R R. Zaky, H M. Abou-El-Nadar, Janet R. Morrow, Nickel (II) complexes as paramagnetic shift and paraCEST agents, Eur. J. Inorg. Chem., doi: 10.1002/ejic.201800021.

29. N. Venugopal, G. Krishnamurthy, H.S. Bhojya Naik, J.D. Manohara, DNA Binding, Molecular Docking and Antimicrobial Evaluation of Novel Azo Dye Ligand and Their Metal Complexes, J. Inorg. Organomet. Polym Mater. 30 (2019) 2608–2625, https://doi.org/10.1007/s10904-019-01394-8

30. KatabathiniNarasimharao, B M. Abu-Zied, Sulaiman Yahya Alfaifi, Cobalt oxidesupported multi wall carbon nanotube catalysts for hydrogen production via sodium

borohydride hydrolysis, Int. J. Hydrog. Energy., 2020, 46, 6404-6418. doi: 10.1016/j.ijhydene.2020.11.112.

31. Harshala Sandip Naik, ParvindarManejarSah, Manali Dhangade, Jaya Lakkakula, RajeshWarluji Raut, Arpita Roy, Saad Alghamdi, Naeem Qusty, Zain Alhindi, Ahmed Kabrah, Anju Rani, Synthesis of a silica matrix with ZnO nanoparticles for the fabrication of a recyclable photodegradation system to eliminate methylene blue dye, De Gruyter, 2023,

0157. https://doi.org/10.1515/gps-2023-0157

31.S. Pramanik, P. Karmakar, Dipak Kumar Das, Electrochemical Sensing of Uric Acid and Guanine Using a Graphite Paste Electrode of NiMn2O4 Spinel Nanoparticles, Biointerface Res. Appl. Chem. 13 (2023) 134, https://doi.org/10.33263/ BRIAC132.134.

32. M. Shabani-Nooshabadi, M. Roostaee, Modification of carbon paste electrode with NiO/graphene oxide nanocomposite and ionic liquids for fabrication of high sensitive voltammetric sensor on sulfamethoxazole analysis, J. Mol. Liq. 220 (2016) 329–333, https://doi.org/10.1016/j.molliq.2016.05.001.

33.A. Nastro, M.P. Germano, V.D. Angelo, A. Marino, M.A. Cannatelli, Extraction methods and bioautography for evaluation of medicinal plant antimicrobial activity, Lett. Appl. Microbiol. 30 (2000) 379–384, https://doi.org/10.1046/ j.1472-765x.2000.00731.x.